The Pennsylvania State University

The Graduate School

Department of Materials Science and Engineering

FABRICATION AND CHARACTERIZATION OF CONDUCTING POLYMER MICROCUPS PRODUCED VIA ELECTROSPINNING AND ELECTROCHEMICAL POLYMERIZATION FOR NEURAL MICROELECTRODES

A Thesis in

Materials Science and Engineering

by

Milad Khorrami

Submitted in Partial Fulfillment
of the Requirements
for the Degree of

Master of Science

December 2015

The thesis of Milad Khorrami was reviewed and approved* by the following:

Mohammad Reza Abidian

Associate Professor of Biomedical Engineering

Thesis Advisor

Ali Borhan

Professor of Chemical Engineering

Esmaila Dabo

Assistant professor of Materials Science and Engineering

Suzanne Mohney

Professor of Materials Science and Engineering and Electrical Engineering
Chair, Intercollege Graduate Degree Program in Materials Science and Engineering

*Signatures are on file in the Graduate School

ABSTRACT

Innovation in the fabrication of implantable micro-scale bioelectronics has been challenging owing to high impedance and low charge storage capacity that result in both low signal-to-noise ratio and low charge injection electrode-tissue interfaces. Additionally, such devices without anti-inflammatory compounds are less likely to maintain their efficacy due to fibrous encapsulation associated with tissue reaction reducing the effective transfer of signals. Thus, there is considerable incentive to fabricate devices capable of delivering therapeutic compounds while maintaining electrical performance. Polypyrrole (PPy) has gained significant interest for biomedical applications owing to its excellent biocompatibility, electrical properties, and mechanical actuation. Poly (lactic-co-glycolic) acid (PLGA) is biodegradable and highly biocompatible, making it an ideal matrix for drug encapsulation. In this research, we have produced hollow PPy cups from template PLGA microspheres on Au electrodes, which were fabricated on Si wafers (two circles with diameters 1.5 and 5.0mm connected with a rectangle 1.0x10mm). Briefly, 4/2wt% PLGA/benzyltriethylammonium chloride was dissolved in chloroform and electrosprayed on the Si electrodes using an applied electrical field of $100kVm^{-1}$. PLGA was then coated with PPy/poly (styrenesulfonate) using electrochemical deposition (current density $0.5mA/cm^2$) for 5 different time durations. The spherical PLGA coated with PPY was then dissolved in chloroform to create hollow PPy cups. These microspherical cups are relatively uniform in size, having average diameters of 3.45±0.31µm, indicating a CV of 9%. Furthermore, Impedance spectroscopy and cyclic voltammetry were performed on all 5 samples and a gold reference to investigate the impedance and charge storage capacity. The size and shape of PPy cups were characterized using Field-Emission SEM. The hollow PPy cups decreased the impedance from 445 ± 63 Ω for bare gold to 354 ± 39 Ω for 8 min PPy-coated electrode, a difference of 20% at 1kHz. The additional surface area obtained by removal of the PLGA cores significantly increased the effective surface area of electrode, thus lowering the impedance. The PPy cups also significantly enhanced the charge storage capacity from 2.5 to $47.5mC/cm^2$; nearly 95%. In conclusion, we successfully demonstrated: (1) electrochemical deposition of PPy around the electrosprayed PLGA microspheres, (2) removal of PLGA microspheres to fabricate hollow PPy cups, and (3) improvement of electrical properties of Au electrodes by decreasing impedance and increasing charge storage capacity. This study demonstrates the potential of our conductive microstructures for neural interfacing and neural regeneration while retaining functionality for drug delivery.

TABLE OF CONTENT

LIST OF FIGURES

LIST OF TABLES

ACKNOWLEDGMENTS

I would like to express my deepest expression to my advisor Dr. Mohammad Reza Abidian for providing me an opportunity to join his lab and also I would like to appreciate for supporting and advising me not only in my research but also in my personal life. I would also thank him for his patience, motivation, and immense knowledge. Without his help I would not be where I am today.

Besides my advisor, I would like to thank to my committee members Dr. Ali Borhan and Dr. Esmaila Dabo for their insightful comments and guidance.

I thank my fellow labmates Martin Antensteiner, Fatemeh Fallahianbijan and Ning Yi in for stimulating discussions, for the sleepless night we were working together before deadlines and all the enjoyable moment that we had together.

I would like to thank Material Science and Engineering department for letting me fulfill my dream of being student at Penn State.

My special thanks to Pouria Motevalian who helped me a lot for settling down in State College and teaching me how to stand on my feet in life. I wish him best of luck in his PhD program.

Last but not least, my parents, who supported me to accomplish my dreams. Thank them for giving me, the most powerful inspiration, guidance, and positive energy by using their experience wisdom. Thanks for talking to me every night while we were far away for thousands of miles.

1. Introduction

The objective of this project is to investigate development of novel conductive biomaterials for neural interface application. In a few past decades, many different kinds of drug encapsulations have been designed. A considerable amount of work has been done to investigate the factors affecting on the biocompatible materials and drug release and how to make them sustainable.[1] An ideal neural interface material performs long-term reliability and unified integration with peripheral nervous system.

In this chapter the advancement of different neural interface biomaterials such as graphene, carbon nanotube, silicon nanowires and conducting polymers have been discussed.

1.1. Reactive tissue response to neural probe

The distance between probe and neurons has significant role on quality and strength of the recording and/or stimulating signals. The amplitude of the neurons reduces briskly as a function of distance from probe. In addition, size of the electrode should be very small in order to minimize brain tissue distortion and maximize the recording signals by lowering the impedance. Hence, it is critical to understand the tissue response to external probe in terms of acute and chronic[2].

1.1.1. Acute Response

Mechanical trauma will trigger the acute response by inserting the electrode in brain tissue. The reason for mechanical trauma is difference in mechanical properties of

brain and metallic electrodes (eg. Young modulus of silicon in 15GPa and young modulus of brain tissue is about 100KPa).[3] As the probe is inserted inside the brain, the neurons might be torn or cut and as a result, the tissue might expand or contradict. In physiological aspect, activated microglia will then reach the injured site to rehabilitate by releasing numerous neurotoxic factors, such as cytokines, chemokines, neurotransmitters and reactive oxygen species. Finally, few neurons can be found around the probe within the 100μm however the density of neurons is normal outside of this killing zone. It takes about 4-6 weeks for neurons to rehabilitate themselves and grow around the inserted probe.[4]

1.1.2. Chronic Response

Chronic response will begin once the acute response drops. This response is characterized by presence of both activated microglia and reactive astrocytes. Microglia then colonies the serum factors including monocyte/macrophage chemotactic proteins on the surface. Furthermore, activated microglia and reactive astrocytes modulate the production of thin layer of ECM proteins, basal lamina that contribute organizing the glial scar.[5] These glial scars significantly increase the impedance of electrodes.

1.2. Biofouling and biological response

When a device is implanted inside the brain, fouling will be happened around the prob. In fact, there is excessive amount of gliosis can be seen at the interface of tissue and device that lowering the connection and decrease the functionality of implant devices such as brain microelectrodes. The thickness of this glial scar might be more than 50 μm and it

has found that this gliotic barrier would significantly decrease the recording and/or stimulating the signals of brain neurons. The strength of this neural picks is extensively influenced by this biofouled layer. In addition, it has been found out that by implanting the external device, there is a dramatically decreasing in in the neural density around the probe that is called “the killing zone”. The killing zone is explained as a region around the external device that amount of existence neurons are 90 % lower than what is expected to be at that place. Also it has been reported that neurons that are located more than 50 μm apart the probe can be hardly be distinguished and those neurons which are located more than 140 μm from probe are not recognized. Therefore, an anti-inflammatory agent is needed order to achieve a long-term stable and efficient electrodes for recording or stimulating from brain[6].

1.3. Materials for Neural Microelectrodes

1.3.1. Conducing Polymer

Neural microelectrodes coated with conducting polymers aim to improve signal quality of recording neural activity and/or stimulating neurons through providing high surface area and low mechanical mismatch between electrodes and brain tissue.[7] Additionally, charge transfer capacity can be improved through reduction of impedance In general, polymers are softer than metallic materials, therefore, it is hypothesized that inflammation around the inserted conducting polymer-coated electrode reduces due to reduction of strain mismatch between electrode and tissue.[8]

Conduction property of these materials owe to presence of conjugated single bound double bound along the polymer backbone. The bonds among the carbons are alternatively single

and double bounds. The single bonds are sigma bond which is relatively strong and also double bonds contain sigma bond in addition "pi" bond that is relatively weak.[9] For making a conducting polymer, dopants introduced to conducting polymer to carry charge in the forms of extra electron. The dopants neutralize the backbone while the conducting polymers are usually oxidized.[10] Biocompatibility of conducting polymer such as polypyrrole (PPY) and effect of different dopants has been characterized by Bakker et al.[11]

1.3.2. Carbon nanotube

Carbon nanotube (CNT) was first introduced in by Iijima in 1991 and first application for CNT was reported as a filler in 1994 by Ajayan et al. CNT has the unique combination of mechanical, electrical, and thermal properties. CNTs are stronger than steel, lighter than aluminum, and more conductive than copper that bring a lot of attention to their applications. For example, experimental results on single wall CNTs show an extremely high young modulus 640 GPa to 1 TPa and a tensile strength of 150 to 180 GPa depending on their structure parameter. CNTs are very good conductors since they can carry electron charges through over long tube length without significant scattering (electron mean free path for metallic material). [12]

CNTs are fabricated through the solution blending, melt blending, and in situ polymerization. CNTs can also be aligned during and after fabrication process using mechanical stretching, spin-casting, wet spinning, melt fiber spinning, and electrospinning.[13]

1.3.3. Graphene

Graphene is the two-dimensional single layer sheet of SP^2-hybride carbon atoms in hexagonal arrangement as it is shown in figure 1-1. It is one of the most promising materials in comparison to CNTs due to its exceptional electronic properties such as no band gap in graphene's structure or ultra-high carrier mobility[14]. Graphene has many applications such as sensors, solar cells, transistors, and capacitors and also in field of biomedical engineering[15].

Graphene structure has long-rang Pi-conjugation that yields extraordinary thermal mechanical and electrical properties. In detail, there is 120 C-C bond angles which have sigma bond together. Carbon has 4 electrons in its valence band. Three of those electrons participate in plane with sigma bond and one electron remains on the top of the carbon that has pi connection or weak Van der Waals bond to another layer of graphene. In addition, the sigma bond is much stronger than Van der Waals bonds. Therefore, graphene's Young modulus in the plane is much higher than perpendicular to plane[16].

Gein and co-workers et al. have invented the first graphene single layer sheet in 2004.[17] There are many different ways for graphene fabrication including chemical vapor deposition (CVD) and epitaxial growth[18].

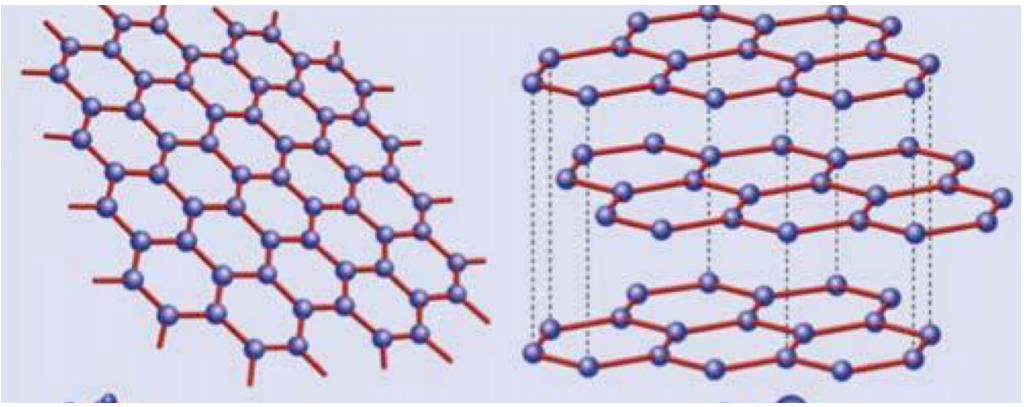

Figure 1-1 Graphene single layer sheet in hexagonal arrangement[19].

Graphene has attracted many interests due to its promising properties such as 1) high electrical conductivity; 2) high elastic modulus; 3) high thermal conductivity (3000W/mK); 4) high electron mobility; 5) large specific area (2600 m^2/gr); and 6) good chemical stability[20].

Graphene oxide is generally produced by the treatment of the graphite using strong mineral acids and oxidation agent, typically via treatment with $KMnO_4$ and H_2SO_4. As a result, delocalization of electron is occurred and the structure of carbon atoms is changed. This occurs at the certain temperature and pressure. There are other ways such as thermal shocking, chemical reduction, CVD (chemical vapor deposition) and etc.[19]. In CVD method, briefly, grapheme procuced from another type of carbon, which is graphite. Graphite is one of the most popular mineral materials. Graphite is placed in the chamber at a high temperature and pressure. Also some gases such as argon and hydrogen should be flowed. Inside the chamber is covered by copper foil. By increasing the temperature and pressure, carbon atoms are evaporated inside the chamber and they deposited on the copper

foil. CVD is more common method for the fabrication of graphene because it is easier process and the produced graphene has better electrical properties .[21]

In 2011 Yao et al. designed the graphene microelectrodes for the first time[14]. They used CVD as the method of fabrication (Figure 1-2). There was a conductive substrate in the bottom that was coated by graphene single layer sheet and PDMS was used for insulating the graphene.

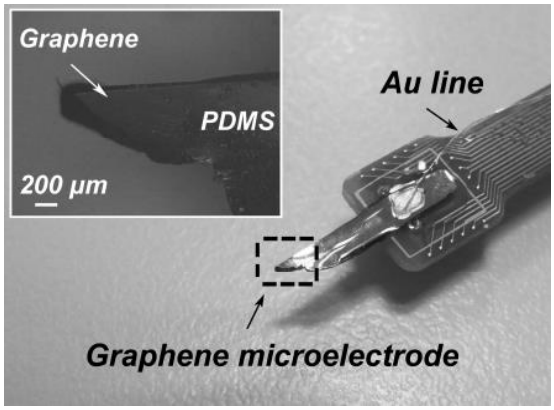

Figure 1-2 Neural microelectrode coated with Graphene for recording and/or stimulating neural activity.[2]

In this research study, the electrical properties of graphene on microelectrodes was measured (Figure 1-3). Two important characterization methods, impedance measurement and cyclic voltammetry, were done. As a result, graphene had very low impedance, high charge density, and high specific capacitance. [19]

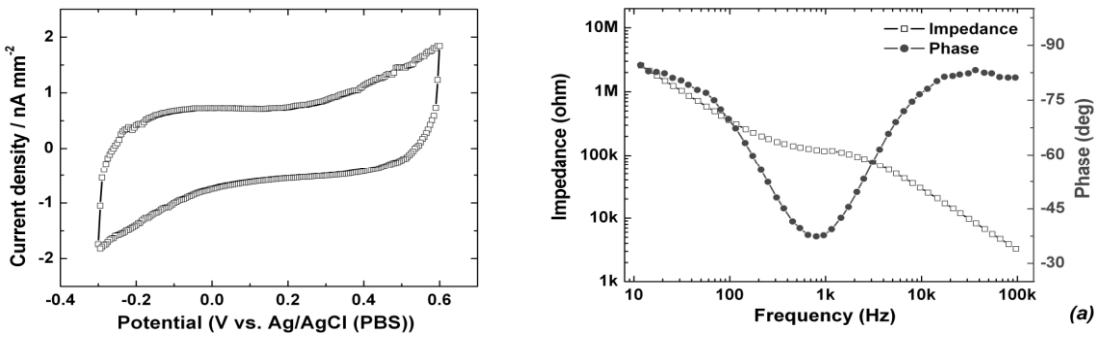

Figure 1-3 Cyclic voltammetry (left) and Impedance measurement (right) for microelectrode coated with Graphene[14].

In the neural recording and stimulation, microelectrodes should be sensitive, selective, and also avoid any tissue damaging. In fact, the material should have low impedance and high injection charge density to be sensitive enough. Moreover, the geometry of the electrode is really critical for the recording. It should be design as smallest as possible to enable communication with individual neurons. Also avoiding tissue damaging is another important factor for the microelectrodes. By implanting the microelectrodes in the brain some tissue displacement might be occurred. In addition, some brain cells might be damaged.[22]

1.3.4. Hybrid Nanomaterials

Hydrogel is a polymeric network which is crosslinked, hydrophilic, and absorbent (they can contain over 90% water).[23] The hydrophilic structure makes it capable of holding large amount of water in its three-dimensional networks[24] (Figure 1-4). Hydrogel has fascinating physical properties such as high water absorbent capacity and colorlessness.

Moreover, the main significant feature of hydrogel is the young modulus. Its young modulus is in KPa range, which is really close to the young modulus of the brain tissue. [25]

Figure 1-4 Hydrogel sample.[26]

In order to have efficient recording microelectrode, it is necessary to employ high a conductive material as well as a soft and flexible material. Therefore, it has been suggested to make a composition of graphene-hydrogel together and using it as a microelectrode.[27]

The composition of graphene and hydrogel has interesting properties such as high conductivity and high flexibility. These two materials can be combined together and can be used for microelectrodes. One of the challenges for designing microelectrodes is to make them more conductive and high flexible. In 2010, the fabrication method of graphene-hydrogel was introduced by Shi et al. for the first time[28]. They represented a unique method to convert the 2D graphene single layer sheet to a 3D structure using the hydrogel. In Fig 1-5, schematic of fabrication and SEM images of graphene-hydrogel are shown. The authors introduced hydrothermal reduction as a method of fabrication. In

summary, as-prepaid graphene and hydrogel were placed at autoclave at high pressure and temperature. Also some additives were added to the composition. Finally they were kept in autoclave for 12 hour and 180C. The composition of graphene-hydrogel can be used not only for microelectrodes but also for self-assemble tissue repair or self-healing tissues[29].

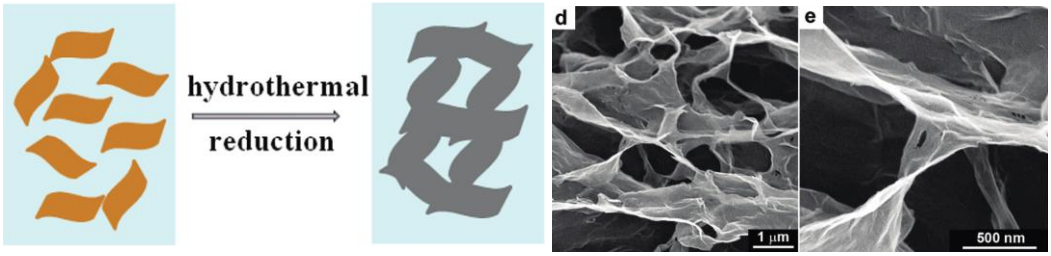

Figure 1-5 Schematic and SEM images of Graphene-Hydrogel structure in two different magnification[29].

Shi et al. have reported lots of application including supercapacitors, sensors, transistors, and microelectrodes for this composition design[29].

Graphene-hydrogel has some significant and interesting electrical and mechanical properties such as high conductivity, low stiffness, and high charge storage density[17]. To measure these properties some experiments have been conducted and also needs to be performed. Impedance measurement and cyclic voltammetry are very important due to their capability of showing electrical properties of this composition. Shi et al. tested the cyclic voltammetry of graphene-hydrogel in 10mV/s and 20mV/s.[28] The surface area inside the curves shows the charge storage capacity of this material. Moreover, impedance measurement was performed and they found the composite had low impedance even

though it was combined with hydrogel. According to the author's hypothesis, using graphene-hydrogel for microelectrodes, this composition should have low impedance and high charge storage capacity as can be seen in figure 1-6.[19]

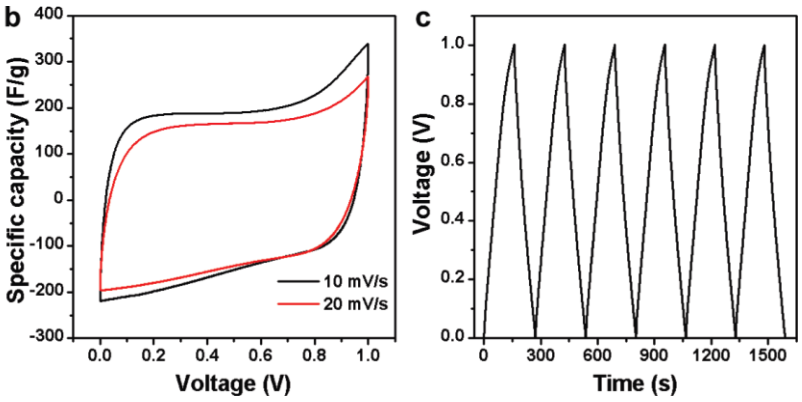

Figure 1-6 cyclic voltammetry measurement of graphene-hydrogel composition in 10 and 20 mV/S CV rate[28].

One of the challenges for neural microelectrodes is to produce a high conductive material that does not cause any tissue damage. This issue can be addressed by both graphene and hydrogel.[30]

1.4. Poly(lactide-co-glycolide)

An extensive amount of researches has been dedicated to investigate the drug delivery with biodegradable polymers.[31] Among various biodegradable polymers, thermoplastics such as PLA and PGA, and co-polymer PLGA has attracted many interests due to their unique physical and chemical properties such as biocompatibility[32], biodegradability, and mechanical strength. In addition, these materials have been approved by Food and Drug

Administration (FDA)[33] for medical applications.[34] In addition, many researches have focused on PLGA due to easy fabrication and ability of carrying different compounds like vaccine, peptide, proteins, and etc[8].

The factors affected in PLGA degradation are shown in table 1-1.

Table 1-1 Factors affecting on chemical and mechanical behavior of biodegradable polymer.[8]

Factors affecting the hydrolytic behavior of biodegradable polymer
- Water permeability and solubility (hydrophilicity/hydrophobicity) - Chemical composition - Mechanism of hydrolysis (noncatalytic, autocatalytic, enzymatic) - Additive (acidic, basic, monomers, solvents, drugs) - Morphology (crystalline, amorphous) - Device dimensions (Size, shape, surface to volume ratio) - Porosity - Glass transition temperature (glassy, rubbery) - Molecular weight and molecular weight distribution - Physico-chemical factors (ion exchange, ionic strength, pH) - Sterilization - Site of implantation

1.5. Polypyrrole

Recently, conducting polymers with conjugated single bonds-double bonds have been attracted many interests due to their promising electrical properties. Among those conducting polymers, polypyrrole (PPY) has been extensively investigated because of its great electrical conductivity, chemical stability, and easy synthesis.[35] It has many applications such as biosensors, batteries, gas sensors, actuators, anti-electrostatic coating, and solid electrolyte capacitors. PPY coating has promising thermal and mechanical stabilities. For example, PPY-based polymer can be used as coating material in order to prevent corrosion of the metals[36].

PPY can be synthetized by either electrochemical or chemical oxidative polymerization.[37] The relationship between the chemical properties of PPY and polymerization condition has been extensively investigated. In 1994, Biswas and Roy focused on the morphology and thermal stability of chemically PPY synthetized ($FeCl_3$ was the dopant) in an aqueous medium. They found that PPY exhibited a spongy texture at 160-170 C glass transition with $3Scm^{-1}$ conductivity[8]. In another study, PPY was prepaid by electropolymerization[38]. They used $Fe_2(SO_4)_3$ as an oxidant and anionic surfactant with different additives in order to enhance the conductivity (Table 2-2).

Table 1- 2 Conductivity of conducting polymers with different oxidant and additive.[37]

Oxidant (mold.m^{-3})	Additive (mold.m^{-3})	Conductivity (S.cm^{-1})
$(NH_4)S_2O_8$ (0.1)	-	4.42
$(NH_4)S_2O_8$ (0.1)	NaDBS (0.0225)	0.57
$(NH_4)S_2O_8$ (0.1)	NaANS (0.024)	0.221
$Fe_2(SO_4)_3$ (0.1)	NaDBS (0.0225)	26.1
$Fe_2(SO_4)_3$ (0.1)	NaANS (0.024)	15.7
$Fe_2(SO_4)_3$ (0.1)	NaAS (0.022)	40.7

2. Materials and Methods

2.1. Materials

PLGA (85:15 LA:GA 7E) with an inherent viscosity of 0.6-0.8 dLg^{-1} was purchased from Evonik Industries (Birmingham, AL). Benzyltriethylammonium chloride (BTEAC) and pyrrole (MW 67.09$gmol^{-1}$) were purchased from Sigma-Aldrich. Poly (sodium-p-styrenesulfonate) (PSS, MW 70 kD) was purchased from Acros-Organics. Chloroform was purchased from SupraSolv Company. N-type Silicon wafer coated by TiO_2 was purchased from University Wafer Company. Spinnerets (metal tip 22 gauge), plastic syringes (3ml), petri dishes (120mm diameter), and plastic microscope slides were purchased from VWR.

2.1.1. PLGA solution

Biodegradable polymer PLGA was solved in chloroform. One of the main parameters effects on result of electrospraying is solution concentration. In fact, percentage of PLGA in chloroform is very critical since it will change the shape of samples from fibers to particles by decreasing the concentration.[39] We have shown that by increasing the PLGA concentration the shape of PLGA was observed as microspheres, beaded microfibers, and microfibers. In this research, the microspheres were desired and we found that the microspheres could be obtained at 4% PLGA in chloroform. Another challenge was the size of microspheres. According to previous research, by adding 2% BTEAC, we could

decrease the size of microspheres. Therefore, 2% BTEAC respect to PLGA was added to the solution.

This project consists of two parts: 1) fabrication of PLGA microspheres followed by PPY coating and 2) removing of PLGA particles to create the hallow PPY microcups.

2.2. Fabrication Method

2.2.1. Fabrication of e Substrates

Gold (Au) electrodes were fabricated on Si wafers (two circles with diameters 1.5mm and 5.0mm connected with a rectangle 1 x 10mm). In order to make the desired pattern, first, a tape was cut using a laser cutter in specific shape and size as mentioned. Then, the tape was placed on the Si wafer. A thin layer of titanium (Ti) (10nm) was deposited to support Au layer (100nm) via evaporation deposition with deposition rate of 1nm/sec. The function of Ti is to support the adhesion of Au on Si wafer.

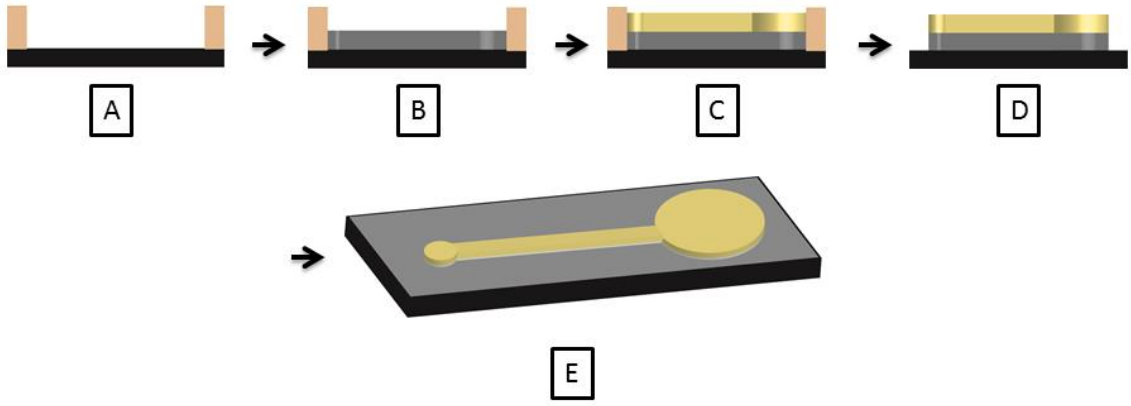

Figure 2-1 Schematic picture of substrate nanofabrication. A) the designed mask was put on Si wafer B)10nm layer of Ti was deposited C)100nm of Au was deposited D) Finally, mask was detached from the surface of Si wafer E) 3D schematic picture nanofabricated substrate. (all the schematic picture were made using Adobe Illustrator software).

2.2.2. Electrospinning

A homogeneous solution of 4wt% (w/w) PLGA with 2wt% BTEAC (w/w with respect to PLGA) was prepared by dissolving 0.617g of PLGA and 0.0123g BTEAC in 10ml of chloroform at room temperature for 12 hours. The mixture was electrosprayed onto the 1.5mm diameter circle on the substrates described above using an applied field of $100kVm^{-1}$ (8kV applied voltage and 8cm distance between syringe needle and substrate) and 500µl/hr flow rate. A tip gauge number 22 was used.

2.2.3. Electrochemical Deposition of Conducting Polymers

The electrochemical polymerization was performed using an Autolab PGSTAT 302N in galvanostatic mode with a two-electrode configuration at room temperature. PLGA microspheres were coated by 0.2 M PPy doped using 0.2M PSS at current density

0.5mA.cm^{-2} over 5 different deposition times (1 to 8min at 2min time intervals). The reference electrode Ag/AgCl and counter electrodes were connected to a platinum wire in the solution.

2.2.4 Removing of PLGA from PPy-coated microspheres

The PPy-coated PLGA microspheres were soaked in chloroform stirred for 12 hrs. We designed the container (figure 2-2) for PLGA dissolving using cupper wires, clamps and glass container. Samples were attached to clamps and they were hanged from container cab for 12 hrs.

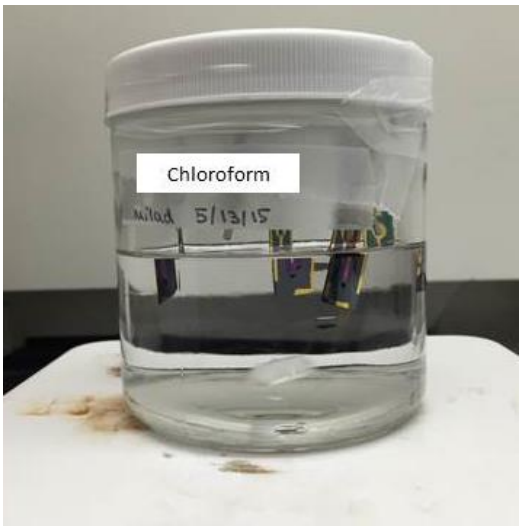

Figure 2-2 Degradation container of Chloroform for PLGA microspheres in order to make a hallow microcups.

2.3. Characterization Method

2.3.1. Electrochemical Impedance Spectroscopy (EIS)

EIS was used to determine the impedance of PPy-coated and Au electrodes. Measurements were done by using an Autolab PGSTAT 302N and Nova Frequency Response Analyzer software in potentiostatic mode. A solution of 0.1M phosphate-buffered saline (PBS, pH=7.4) was used as the electrolyte in a three-electrode configuration. The Ag/AgCl reference electrode, PPy-coated microspheres, and the counter electrode were immersed in the electrolyte solution. AC sinusoidal signal with10mV rms amplitude was imposed to measure the impedance magnitude and phase angel over a frequency range of $1\text{-}10^4$ Hz.

2.3.2. Cyclic Voltammetry (CV)

A staircase CV was performed in the three-electrode configuration using the Autolab. The potential on working electrode was swept from -0.8 to 0.4 V versus Ag/AgCl reference electrode at a scan rate of 30mV s^{-1}. In order to calculate the charge storages capacity the first stable cycle was used.

2.3.3. Size and Morphology

To characterize the size, and morphology of the electrosprayed PLGA microspheres and hollow PPy microcups, optical images were taken at 50X magnification (Zeiss Imager Z1, Germany) and analyzed using Axiovision digital processing software. After PPy coating, the conductive microstructures were mounted on aluminum stubs using carbon tape, and sputter coated by gold (Denton Sputter Coater) for 40s in 40mA in order to reduce charging. The morphology of the PPy coatings on PLGA microspheres was characterized using Field Emission Scanning Electron Microscopy (FESEM) (FEI Helios NanoLab 660 FIB/FESEM) at two different magnifications (7.5K and 32.5K). The height of PPy coating on the PLGA microspheres and the opening diameter of the PPy microcups were analyzed with ImageJ analysis software.

2.3.4. Statistical Analysis

Statistical analysis of the electrosprayed microspheres (n=200) was performed by standard statistical analysis (Origin 8.6 SRO, Northampton, MA). Outliers were detected by use of a Grubbs Test with a significance of 0.05 (standard two-sided analysis). Analysis of coating height on the microspheres and opening diameter of the PPy coating was also performed using the same analysis in Origin (n=50 for each coating time).

3. Results and discussions

3.1. Electrospraying

In electrospraying technique different variables have extensive effect on size and shape of particles. In this section, influence of solution concentration, flow rate, voltage, and distance were measured and compared. The standard parameters are written in table

Table 3-1 Standard parameters of electrospinning for test matrix experiments. This parameters were set and effect of each one has been measured.

Electrospinning parameters	Experiment standard value
Voltage	8KV
Distance	8cm
Flow rate	500μL/hr
Tip gauge	22
PLGA Concentration	4%

3.1.1. Effect of Solution Concentration

Figure 3-1 shows the particle diameter versus PLGA concentration. This graph indicates that by increasing PLGA concentration, particle size also increases. It was noted that there was fiber formation at 5% and 6% PLGA (Figure 3-2).

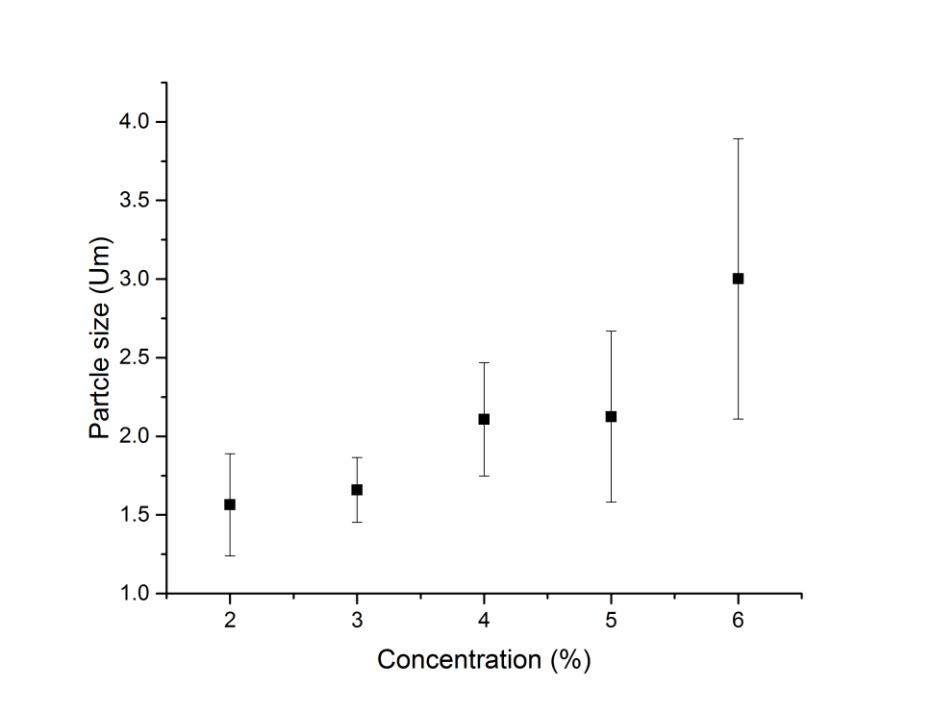

Figure 3-1 PLGA concentration vs. measured particle diameter at voltage of 5KV, working distance of 8cm, tip gauge number 22 and flow rate of 500µL/hr.

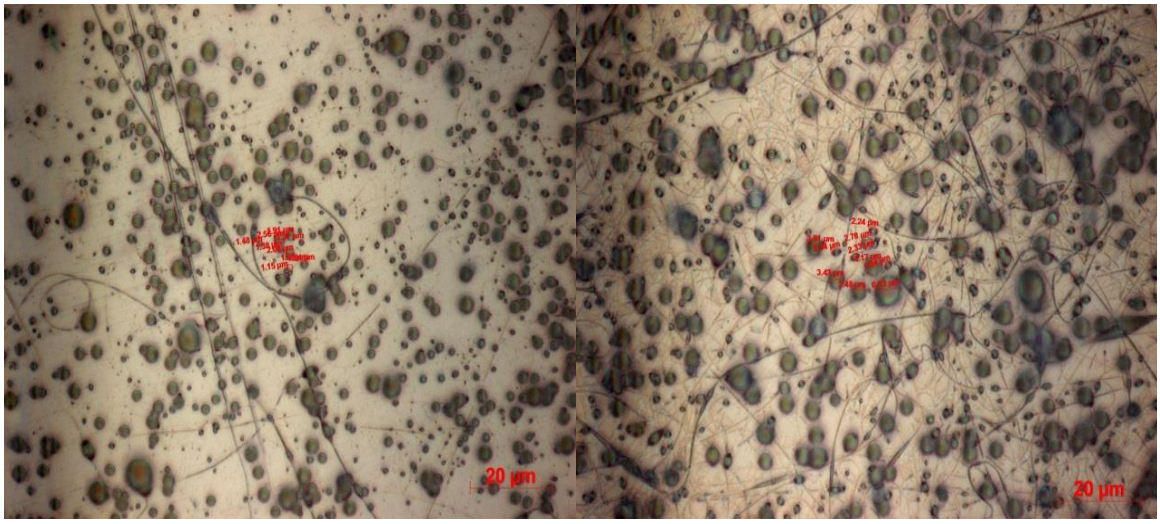

Figure 3-2 Optical microscopy images at 100X of 5% (left) and 6% (right) PLGA in Chloroform solution in electrospinning.

This result is to be expected, as Abidian *et al*.[40] indicated that increasing the PLGA concentration will stimulate the production of microfibers on the substrate. In this project, the goal was to make particle. Therefore, we chosed 4% PLGA respect to chloroform.

3.1.2. Effect of Flow Rate

While flow rate of polymer solution is one of the parameters in electrospinning, it does not have extensive influence on the particle size as it is shown in figure 3-3 because the results show overlapping in different flow rates. Flow rates were established at 250, 500, 750, and 1000 μL/hr.

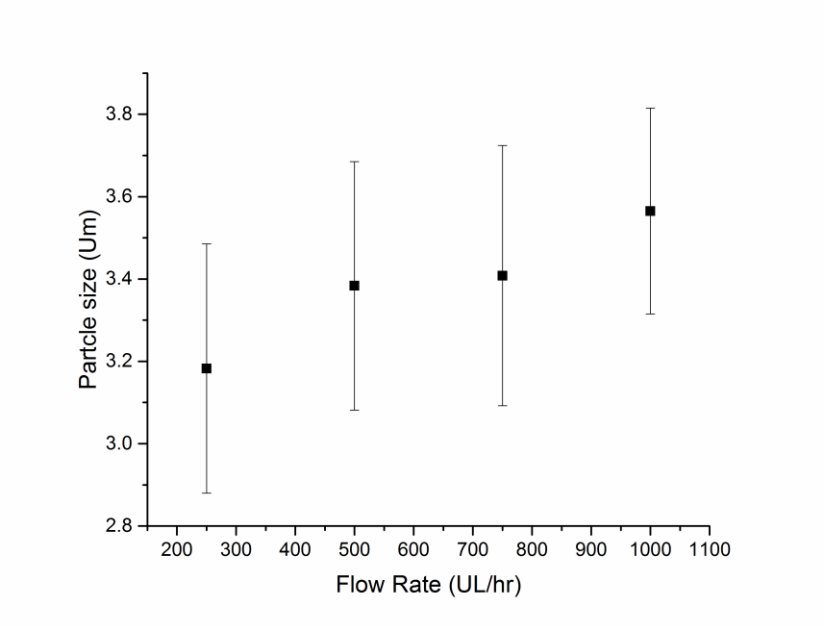

Figure 3-3 Flow rate vs. measured particle diameter at voltage of 5KV, working distance of 8cm, tip gauge number 22 and concentration of 4% PLGA.

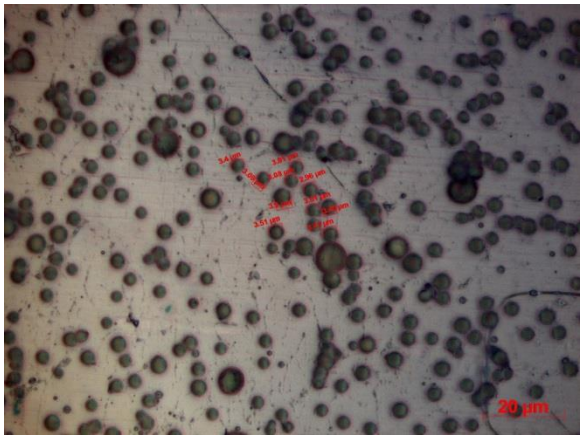

Figure 3-4 Optical microscopy image in 100X at 250µL/hr flow rate in electrospinning.

3.1.3. Effect of Voltage

Voltage is another parameter in electrospinning. The voltage was varied from 8kV to 16kV. According to the results shown in Figure 3-5, there is an inverse relationship between the voltages to particle diameter. As the voltage increased, the diameter of the particle decreased. The increasing of voltage also led to the production of microfibers. These microfibers can be seen in Figures 3-6.

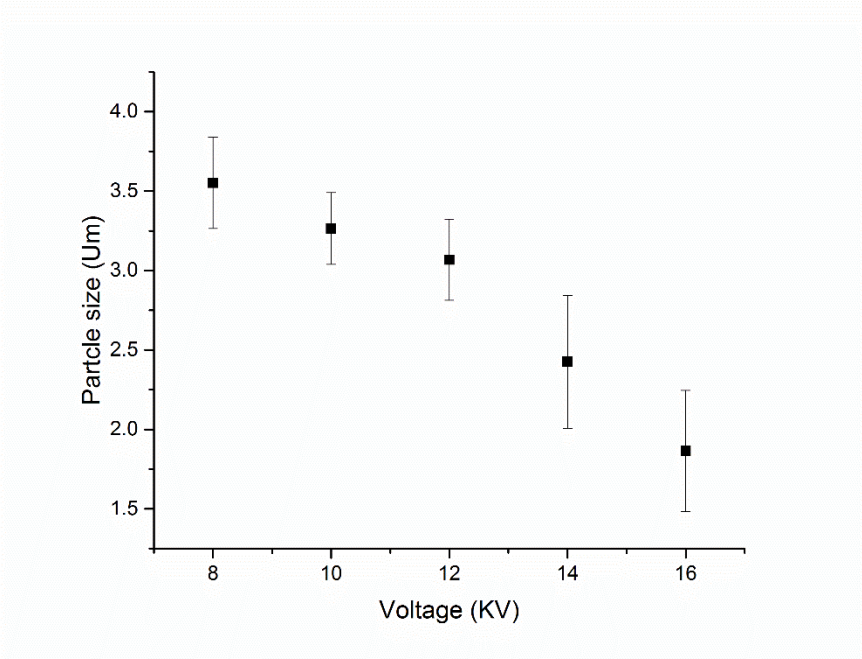

Figure 3-5 Voltage through the sample vs. particle diameter at PLGA concentration of 4%, working distance of 8cm, tip gauge number 22 and flow rate of 500µL/hr.

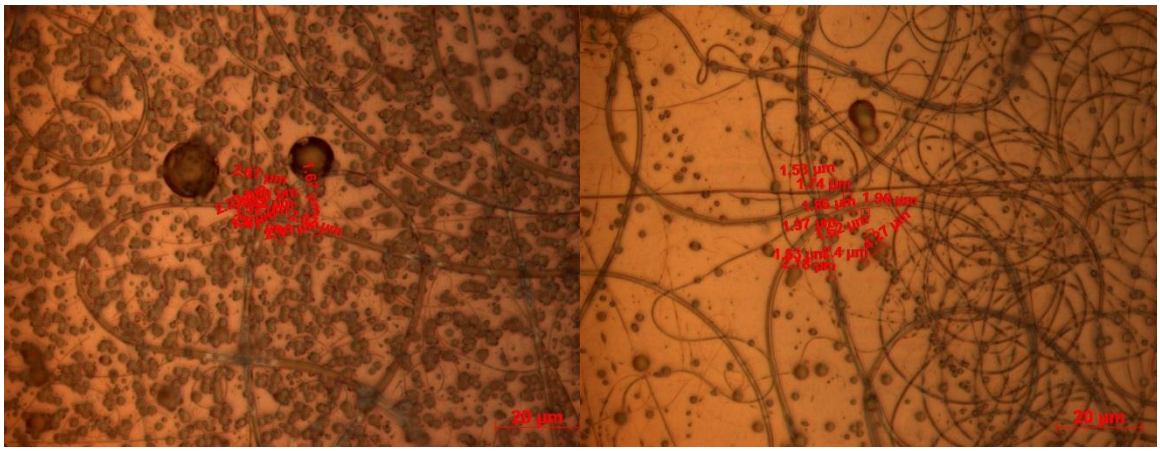

Figure 3-6 Optical microscopy images at 100X of PLGA at voltage of 14 KV (left) and 16kV (right) in electrospinning.

Interestingly, increasing the voltage seemed to produce favorable conditions to produce microfibers. As Figure 3-6 indicates, microfibers were produced as the voltage increased to 14kV and 16kV.

3.1.4. Effect of Distance

The distance from syringe tip to the substrate was changed and particle sizes were measured. Figure 3-7 shows that there was no significant role of distance on particle size. However, lowering the distance to 4.5 cm produced a notable number of fibers. These fibers can be seen below in Figure 3-8. We chose 8cm working distance because of convenient of working with our electrospinning setup.

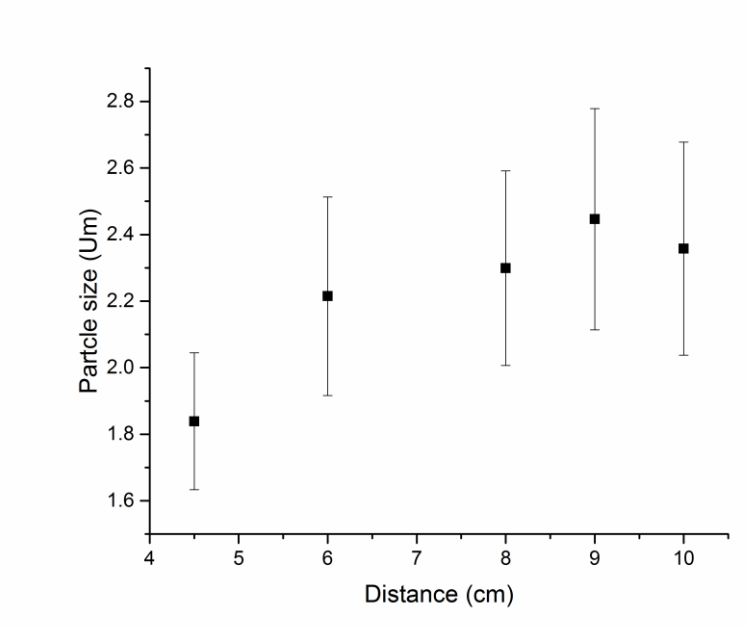

Figure 3-7 Distance from syringe tip to substrate vs. particle size at voltage of 5KV, PLGA concentration of 4%, tip gauge number 22 and flow rate of 500µL/hr.

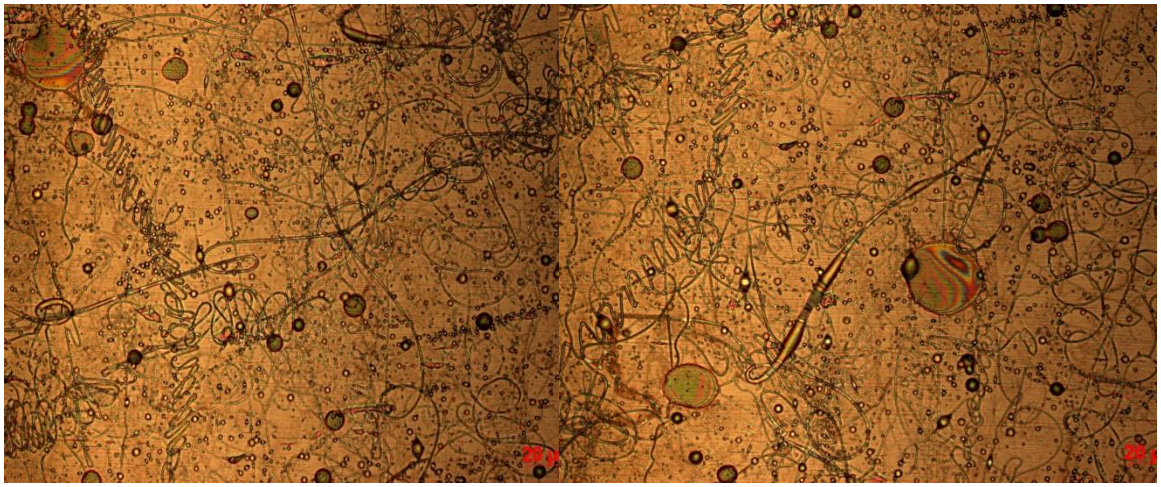

Figure 3-8 100x Magnification of PLGA at 4.5 cm (left) and 6 cm (right) in electrospinning.

3.2. Particle sizes and dispersion

As the histogram is shown in figure 3-9, the particle size ranged from 2.8μm to 3.8μm.

These microspheres were relatively uniform in size, having average diameters of 3.23±0.31μm, indicating a coefficient variation of 9%.

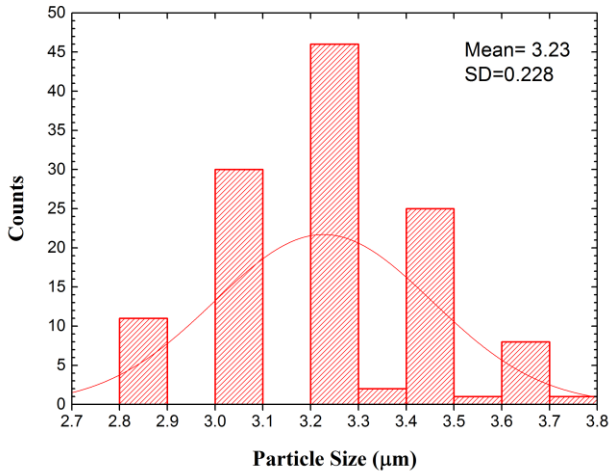

Figure 3-9 histogram diagrams of uncoated PLGA particles with means of 3.23μm and CV of 9%.

3.3. FESEM images of coated PLGA microspheres

The progression of the PPy coating on the PLGA microspheres was analyzed via FESEM and is shown in Figure 3-10. The darks spots and wrinkles on the surface of PLGA microspheres in Figure 3-10 were likely due to charging and electron beam damaging during FESEM. As shown in Fig. 3-10, PPy initially coated the gold substrate. This is because the electrochemical polymerization process occurred at the interface of a conductive substrate and the monomer solution. Since the PLGA microspheres were none conductive, PPy deposited first on the gold substrate and subsequently grew around the PLGA microspheres until only a small gap remained at 6min coating time (Fig 3-10). By 8 minutes of coating, most of the microspheres were completely coated.

-	Low magnification	High magnification
Uncoated sample	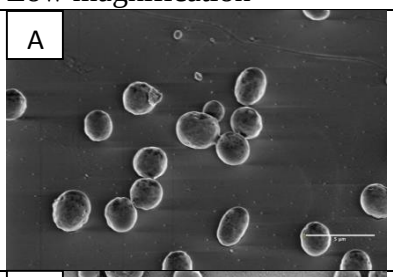	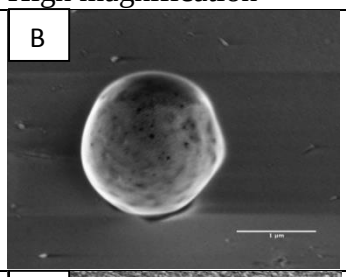
1 min coating	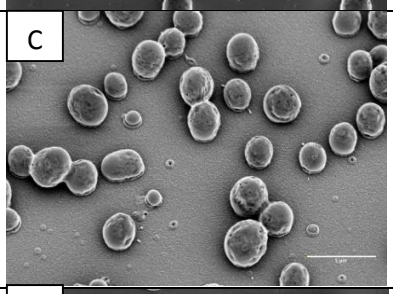	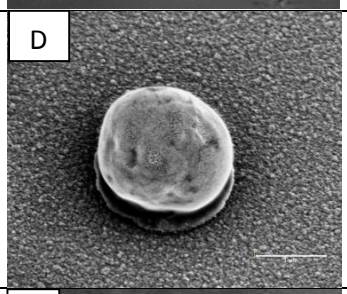
2 min coating	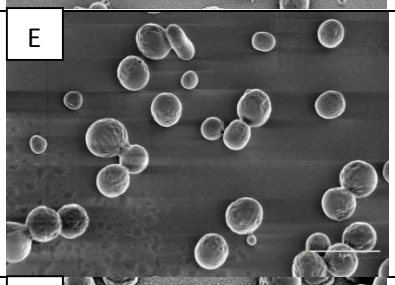	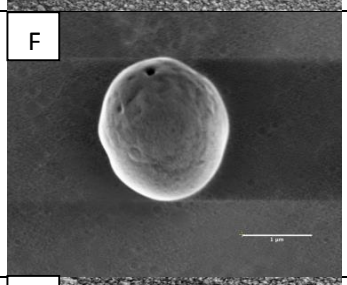
4 min coating	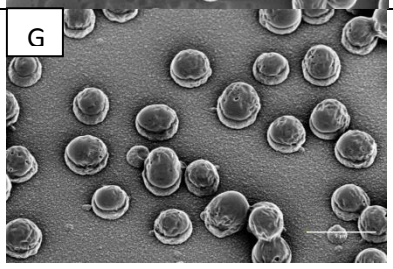	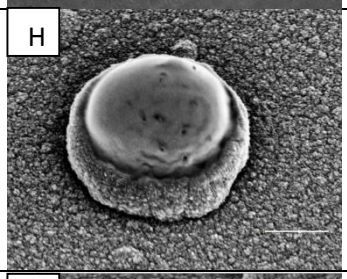
6 min coating	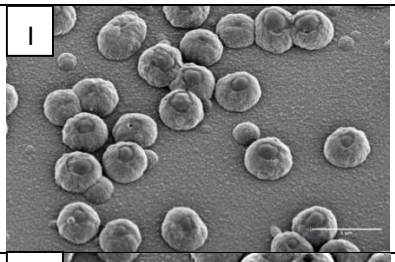	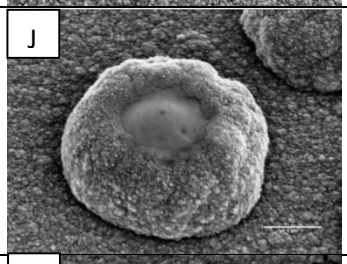
8 min coating	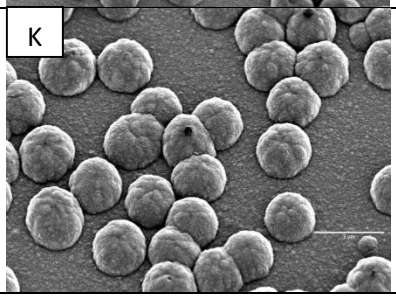	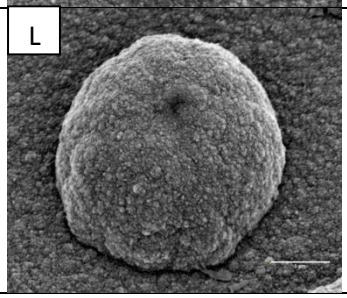

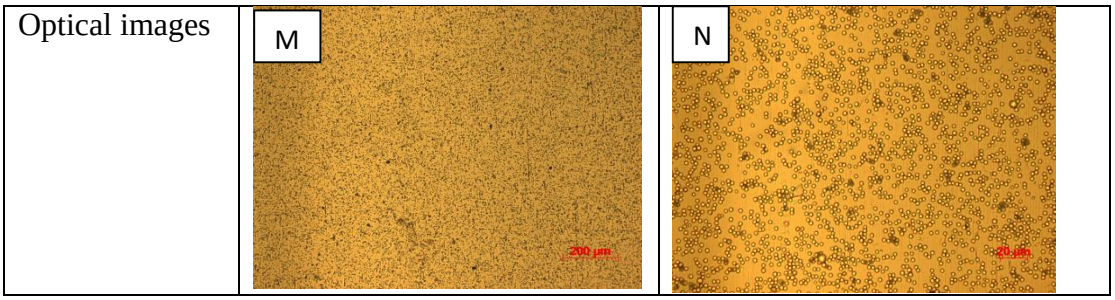

Figure 3-10 Optical microscopy and FESEM images showing PPy coating progression on PLGA microspheres in low and high magnification. a) Electrospinning of BTEAC-loaded PLGA microspheres at low magnification and b) High magnification of electrosprayed PLGA. c) Electrochemical polymerization of PPy. Scales bars: 1µm. Images in the right column are high magnifications of images in the left column, C,D) 1 min coating. E,F) 2 min coating. G,H) 4min coating. I,J) 6min coating. K,L) 8min coating. M,N) Optical microscopy images. Error bars on the left and right column is 1µm and 5µm, respectively except optical images.

3.4. Size and dispersion of coated particles

Figure 3-11, histogram of fully coated particles with a mean value of 3.4µm is shown. Most of the particles were homogeneous in size. The average diameter of coated particles was larger than uncoated particles. The thickness of PPy coating was 0.15µm.

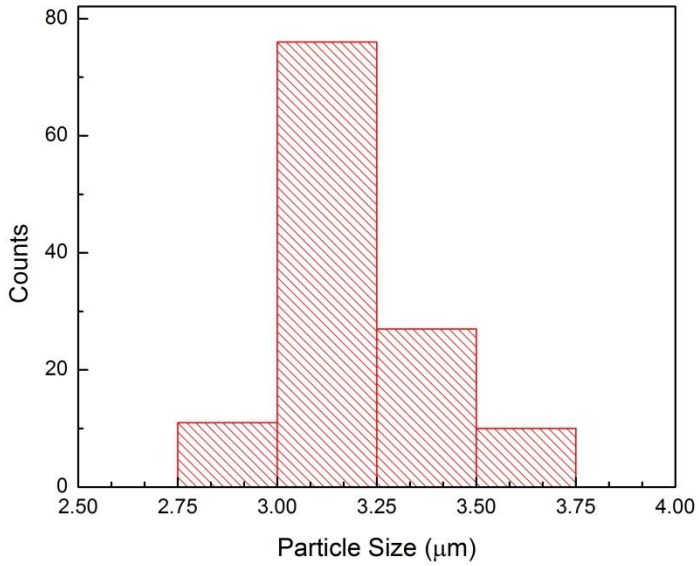

Figure 3-11 Histogram graph of PPy fully covered particles coated with PPY.

According to figure 3-12, by increasing the deposition time, the height of the PPy coating around the particles increased. The height of PPy growth from 1 min to 5 min was linear, however a huge difference was observed between 5 to 6min time depositions. In 8 min coating the entire of particles were covered completely.

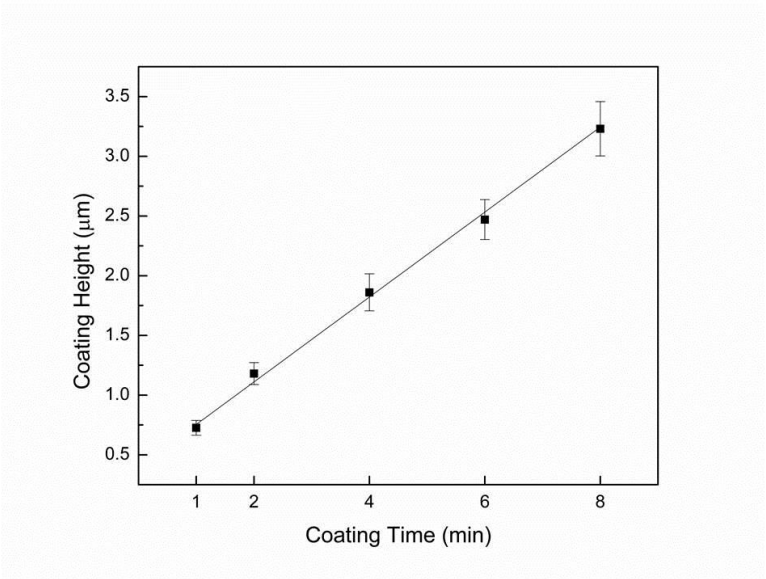

Figure 3-12 Plot showing PPy coating height on PLGA microspheres versus coating time.

The opening diameter of the PPy coating represents the fraction of the PLGA microsphere that was uncoated at the end of the electrochemical polymerization. The results are shown in Figure 3-13. By coating particles from 1 min to 4 min top opening diameter was increased because coating nucleation started from surface of substrate to biggest circle of spheres. After 4min coating, top opening was decreased until particles got fully covered with conducting polymer in 8min.

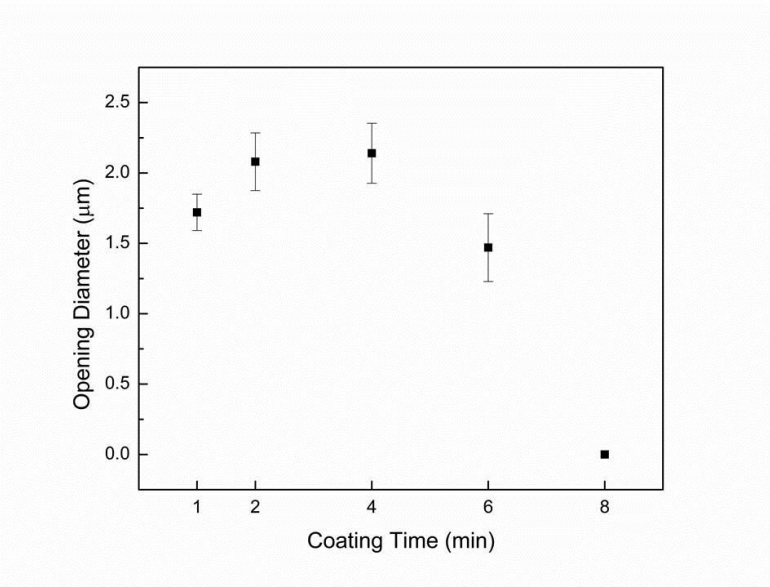

Figure 3-13 Plot showing diameter in μm of PPy coating opening on PLGA microspheres versus coating time.

3.5. FESEM images of hallow PPY microstructures

Subsequent removal of the PLGA template microspheres via chloroform resulted in PPy hollow microstructures, or "microcups" (Figure 3-14). Interestingly, the removal of PLGA enabled the observation of both sides of PPy walls of the microcups themselves and the gold substrate that was covered by PLGA. A detailed analysis of the PPy height and opening diameter was performed and was shown in Figure 3-12 and 3-13. The plot in Figure 3-12 shows a linear trend in PPy coating height as a function of time.

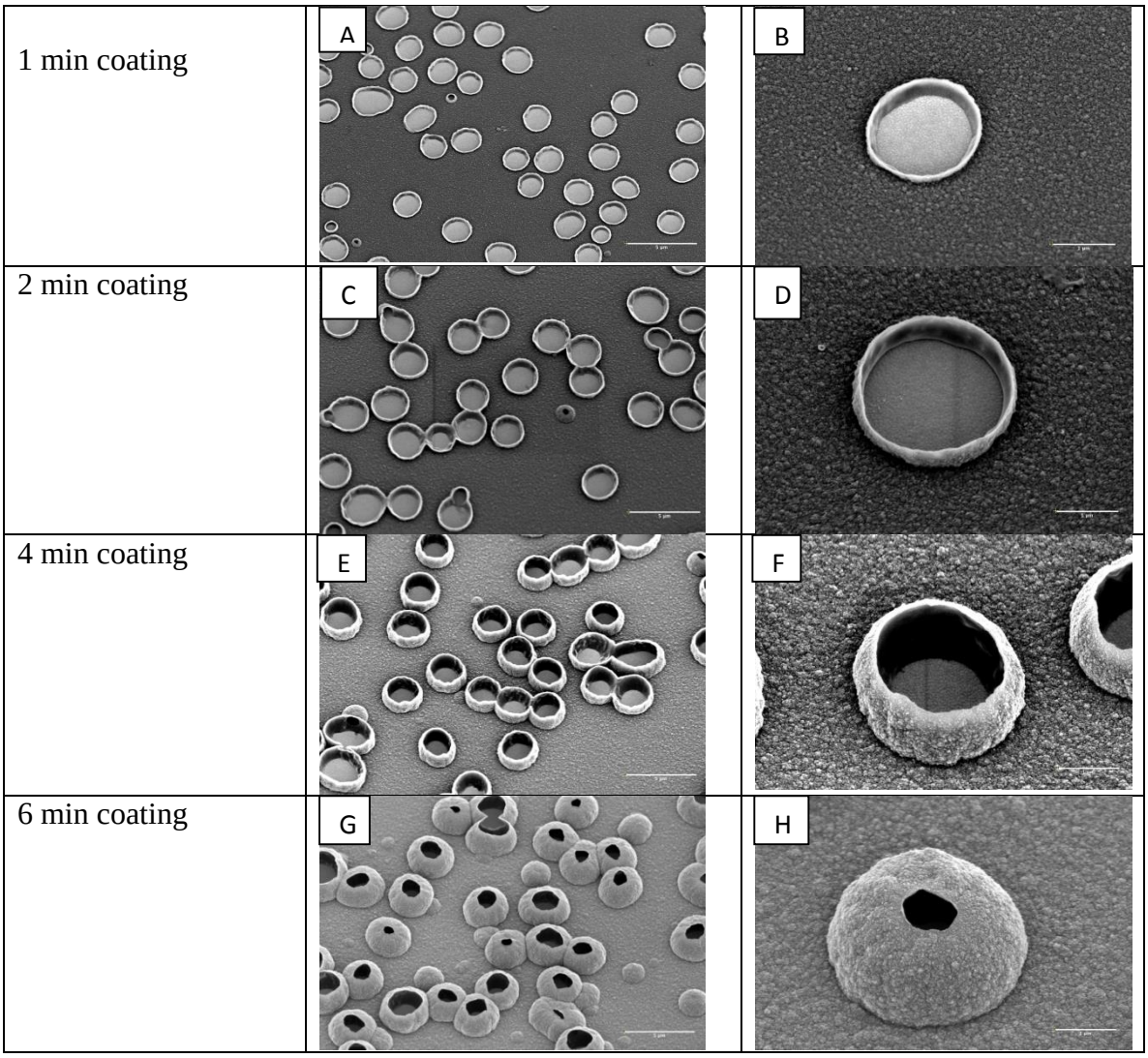

Figure 3-14 FESEM images of PPy hollow cup microstructures after removal of the PLGA template microspheres. Scale bars: 1µm. Images in the right column are high magnifications and low images on the left column. A,B) 1 min coating. C,D) 2 min coating. E,F) 4min coating. G,H) 6min coating. Error bars on the left and right column is 1µm and 5µm, respectively.

Figure 3-15 shows schematic pictures of all steps for making microcups.

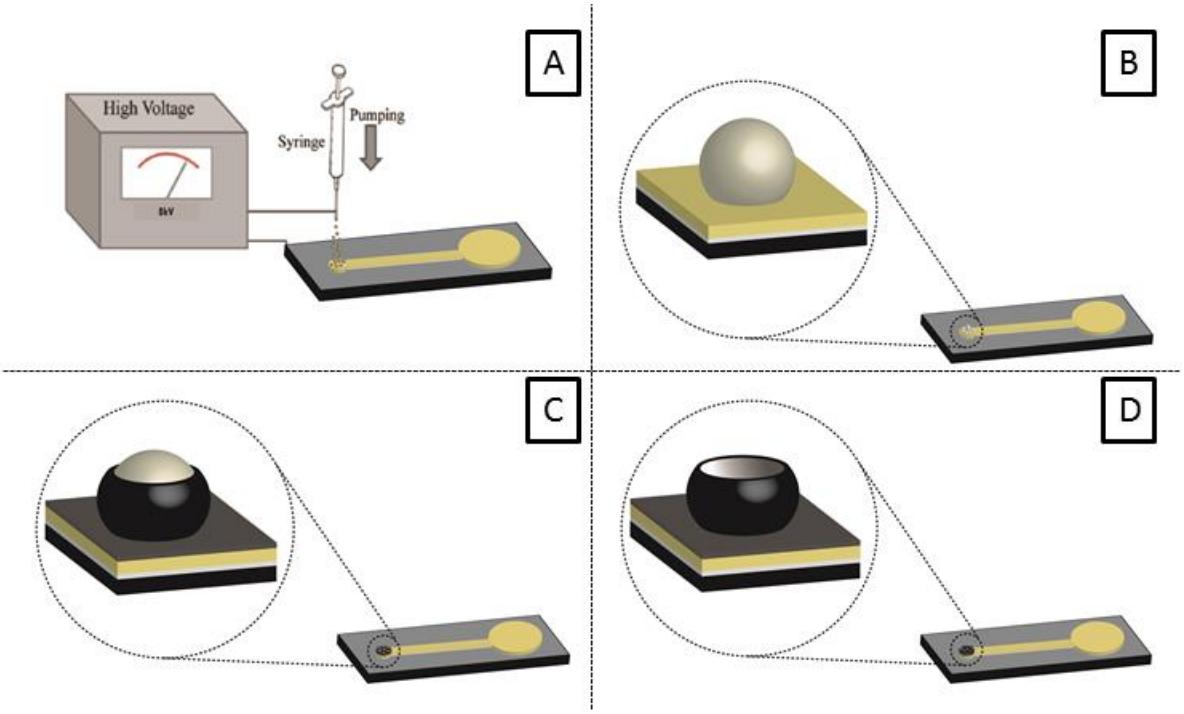

Figure 3-15 Schematic picture of making microcups A) Electrospinning of PLGA solution on nanofabricated substrate B) PLGA particles are electrosprayed on Si wafer C) PPy was electropolymerized around the PLGA particles D) PLGA core was removed and PPy hollow structure was made (All the schematic pictures were made using Adobe Illustrator software).

3.6. Electrochemical Impedance Spectroscopy (EIS)

Figure 3-16 demonstrates the EIS results as a function of frequency for 6 various deposition times. For both bare gold and modified electrodes, it was found that in high range frequency the impedance magnitude decreased, due to the dominant behavior of resistance part of the impedance. However, at low frequencies the capacitance behavior of impedance is more distinguishable. Additionally, the impedance of PPy-coated electrodes was lower than the bare gold across all frequencies..

As shown in Figure 3-17, the impedance of coated and uncoated samples was compared together at 1000 Hz. It was found that by increasing the coating time, the impedance decreased (bare gold electrode from 445.32 ± 63.85 Ω to 354.24 ± 39.71 Ω for 8 min PPy coating).

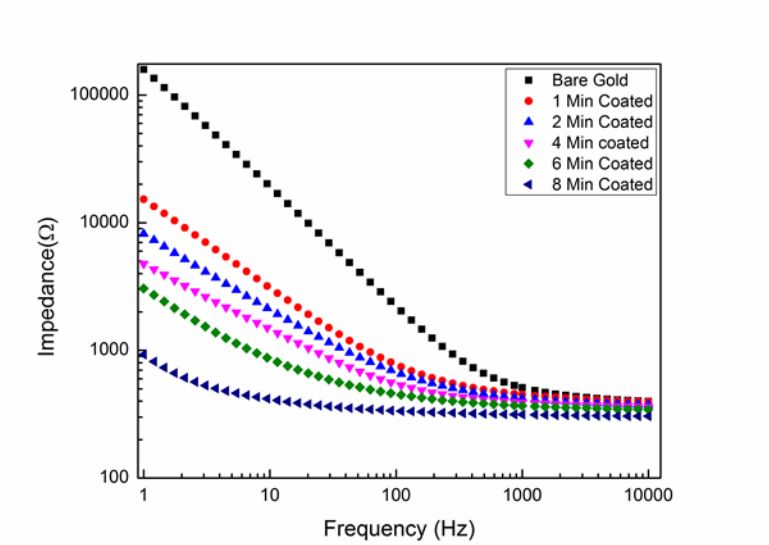

Figure 3-16 Impedance spectroscopy measurement of bare gold and coated particles from 1 min to 8 min with 2 min time intervals.

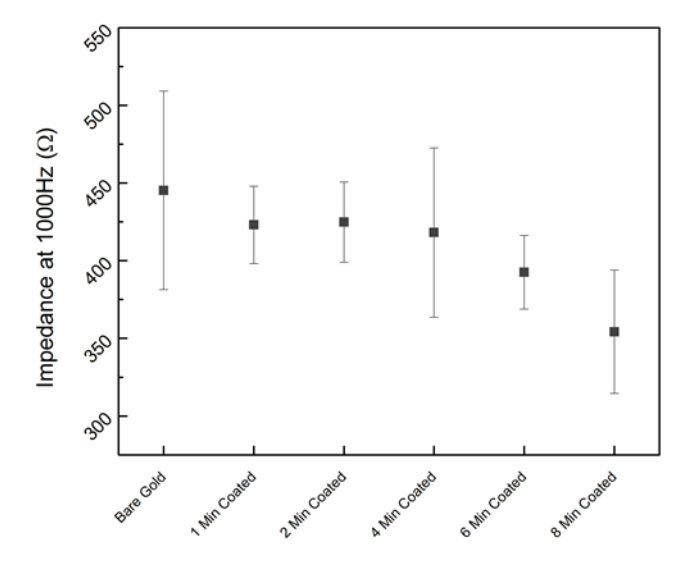

Figure 3-17 Impedance spectroscopy measurement at 1000Hz for bare Gold and coated particles from 1 min to 8 min.

3.7. Cyclic Voltammetry (CV)

Potentiostatic Cyclic Voltammetry staircase was used to determine the charge storage capacity of bare gold and coated electrodes. Figure 3-18 shows CV measurements for Au and PPy coated -particles. The charge storage capacity is directly related to the surface area of CV graph. As shown in Figure 3-19 the charge storage capacity was increased by increasing the coating time. Furthermore, charge capacitance increased from 2.04 ± 0.78 $mC.cm^{-2}$ for bare gold to 48.03 ± 2.79 $mC.cm^{-2}$ for 8 min coated electrode.

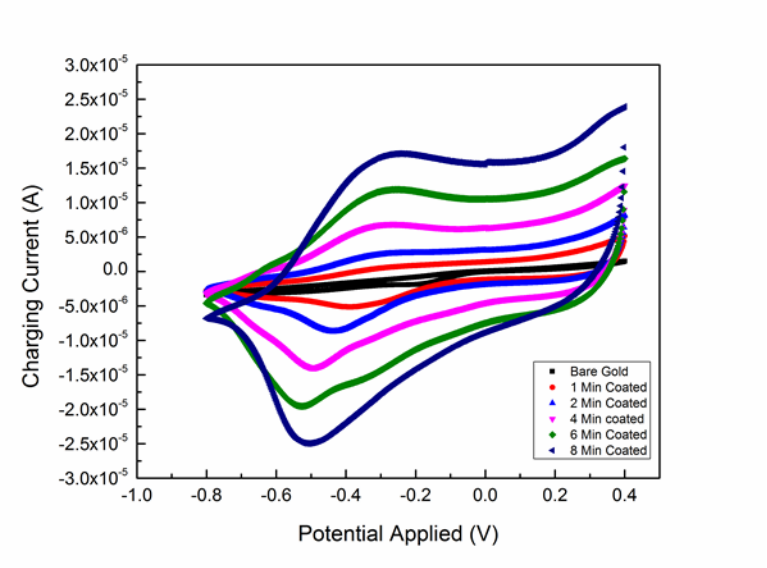

Figure 3-18 Cyclic voltammetry measurement of bare gold and coated particles from 1 min to 8 min with 2 min time intervals.

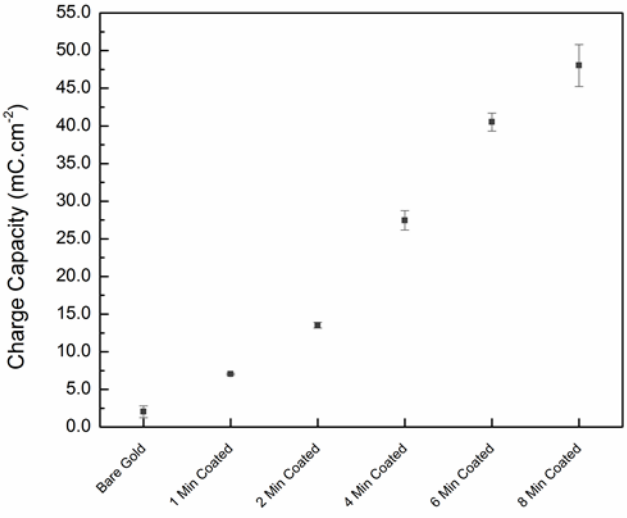

Figure 3-19 Charge storage capacity of bare Gold and coated particles measured by calculating the closed surface area of cyclic voltammetry.

4. Future Directions

In this research, we have successfully shown fabrication process of hallow PPy microcups using PLGA microsphere templates. PPy has been chosen as conducting polymer due to its unique electrical property and convenient fabrication procedure.

In the future, we plan to incorporate drug and biomolecules such as dexamethasone and nerve growth factor (NGF) and release them from conducting polymer microcontainers. These compounds can be loaded inside the PLGA microspheres. By making PLGA microspheres with conducting polymer, it is possible to control the release of the drugs. One of the main challenges for drug delivery is the burst effect. It is predicted by controlling the amount of PPy coating around the PLGA microspheres, we may overcome burst effect challenge.

In addition, the author suggests working on aligned nanofibers loaded with NGF to control the release of drug and guide growth direction of cells.

Moreover, Using Poly(3,4-ethylenedioxythiophene) (PEDOT) as conducting polymer might bring attractions due to its significant electrical properties. PEDOT has better conductivity in compare to PPy.[19] It is suggested to work with PEDOT instead of PPy to measure effect of various conducting polymer on Impedance spectroscopy and charge storage capacity.

References

1. Auras, R., Harte, B. & Selke, S. An Overview of Polylactides as Packaging Materials. *Macromol. Biosci.* **4,** 835–864 (2004).

2. Fattahi, P., Yang, G., Kim, G. & Abidian, M. R. A Review of Organic and Inorganic Biomaterials for Neural Interfaces. *Adv. Mater.* **26,** 1846–1885 (2014).

3. Bledzki, a. K. & Gassan, J. Composites reinforced with cellulose based fibres. *Prog. Polym. Sci.* **24,** 221–274 (1999).

4. Su, Y. *et al.* Controlled release of bone morphogenetic protein 2 and dexamethasone loaded in core–shell PLLACL–collagen fibers for use in bone tissue engineering. *Acta Biomater.* **8,** 763–771 (2012).

5. Gil, E. S. & Hudson, S. M. Stimuli-reponsive polymers and their bioconjugates. *Prog. Polym. Sci.* **29,** 1173–1222 (2004).

6. Kim, D.-H. & Martin, D. C. Sustained release of dexamethasone from hydrophilic matrices using PLGA nanoparticles for neural drug delivery. *Biomaterials* **27,** 3031–3037 (2006).

7. Hutmacher, D. W. Scaffolds in tissue engineering bone and cartilage. *Biomaterials* **21,** 2529–2543 (2000).

8. Jain, R. a. The manufacturing techniques of various drug loaded biodegradable poly(lactide-co-glycolide) (PLGA) devices. *Biomaterials* **21,** 2475–2490 (2000).

9. Baek, S., Green, R. a. & Poole-Warren, L. a. The biological and electrical trade-offs related to the thickness of conducting polymers for neural applications. *Acta Biomater.* **10,** 3048–3058 (2014).

10. Green, R. a., Lovell, N. H., Wallace, G. G. & Poole-Warren, L. a. Conducting polymers for neural interfaces: Challenges in developing an effective long-term implant. *Biomaterials* **29,** 3393–3399 (2008).

11. Fahlgren, A. *et al.* Biocompatibility of Polypyrrole with Human Primary Osteoblasts and the Effect of Dopants. *PLoS One* **10,** e0134023 (2015).

12. Ahn, H.-S. *et al.* Carbon-nanotube-interfaced glass fiber scaffold for regeneration of transected sciatic nerve. *Acta Biomater.* **13,** 324–334 (2015).

13. Mohammad, M. & Winey, K. I. Polymer Nanocomposites Containing Carbon Nanotubes. *Macromolecules* **39,** 5194–5205 (2006).

14. Chen, C. H. *et al.* A graphene-based microelectrode for recording neural signals. *2011 16th Int. Solid-State Sensors, Actuators Microsystems Conf. TRANSDUCERS'11* 1883–1886 (2011). doi:10.1109/TRANSDUCERS.2011.5969794

15. Huang, X. *et al.* Graphene-based materials: Synthesis, characterization, properties, and applications. *Small* **7,** 1876–1902 (2011).

16. Allen, M. J., Tung, V. C. & Kaner, R. B. Honeycomb carbon: A review of graphene. *Chem. Rev.* **110,** 132–145 (2010).

17. Castro Neto, a. H. . *et al.* The electronic properties of graphene. *Rev. Mod. Phys.* **81,** 109–162 (2009).

18. Park, S., Ruoff, R. S. & Engineering, M. Chemical methods for the production of graphenes. *Nat. Nanotechnol.* **4,** 217–24 (2009).

19. Kuilla, T. *et al.* Recent advances in graphene based polymer composites. *Prog. Polym. Sci.* **35,** 1350–1375 (2010).

20. Kim, H., Abdala, A. a. & Macosko, C. W. Graphene/Polymer Nanocomposites. *Macromolecules* **43,** 6515–6530 (2010).

21. Zhang, X. *et al.* Mechanically strong and highly conductive graphene aerogel and its use as electrodes for electrochemical power sources. *J. Mater. Chem.* **21,** 6494 (2011).

22. Li, W. J., Laurencin, C. T., Caterson, E. J., Tuan, R. S. & Ko, F. K. Electrospun nanofibrous structure: A novel scaffold for tissue engineering. *J. Biomed. Mater. Res.* **60,** 613–621 (2002).

23. Jin, R. & Dijkstra, P. J. Hydrogels for Tissue Engineering. *Chem. Rev.* **101,** 1869–1879 (2001).

24. Ahmed, E. M. Hydrogel: Preparation, characterization, and applications: A review. *J. Adv. Res.* **6,** 105–121 (2015).

25. Nair, L. S. & Laurencin, C. T. Biodegradable polymers as biomaterials. *Prog. Polym. Sci.* **32,** 762–798 (2007).

26. Films, G. H. *et al.* Flexible Solid-State Supercapacitors Based on Three-Dimensional. 4042–4049 (2013).

27. Mohanty, a. K., Misra, M. & Hinrichsen, G. Biofibres, biodegradable polymers and biocomposites: An overview. *Macromol. Mater. Eng.* **276-277,** 1–24 (2000).

28. Xu, Y., Sheng, K., Li, C. & Shi, G. Self-assembled graphene hydrogel via a one-step hydrothermal process. *ACS Nano* **4,** 4324–4330 (2010).

29. Hou, C., Duan, Y., Zhang, Q., Wang, H. & Li, Y. Bio-applicable and electroactive near-infrared laser-triggered self-healing hydrogels based on graphene networks. *J. Mater. Chem.* **22,** 14991 (2012).

30. Toshima, N. & Ichikawa, S. Conducting Polymers and Their Hybrids as Organic Thermoelectric Materials. *J. Electron. Mater.* **44,** 384–390 (2015).

31. Yoshimoto, H., Shin, Y. M., Terai, H. & Vacanti, J. P. A biodegradable nanofiber scaffold by electrospinning and its potential for bone tissue engineering. *Biomaterials* **24,** 2077–2082 (2003).

32. Biscazzo, S., Vittadello, M., Lavina, S. & Noto, V. Di. Synthesis and structure of electrolytic complexes based on a -hydro- w -oligo (oxyethylene) hydroxy- poly [oligo (oxyethylene) oxydimethylsililene] and d -MgCl 2. **147,** 377–382 (2002).

33. Panyam, J. & Labhasetwar, V. {B}iodegradable nanoparticles for drug and gene delivery to cells and tissue. *Adv. Drug Deliv. Rev.* **55,** 329–347 (2003).

34. Rezwan, K., Chen, Q. Z., Blaker, J. J. & Boccaccini, A. R. Biodegradable and

bioactive porous polymer/inorganic composite scaffolds for bone tissue engineering. *Biomaterials* **27,** 3413–3431 (2006).

35. Uhrich, K. E., Cannizzaro, S. M., Langer, R. S. & Shakesheff, K. M. Polymeric systems for controlled drug release. *Chem. Rev.* **99,** 3181–98 (1999).

36. Wang, L.-X., Li, X.-G. & Yang, Y.-L. Preparation, properties and applications of polypyrroles. *React. Funct. Polym.* **47,** 125–139 (2001).

37. Armand, M. B. Polymer Electrolytes. *Annu. Rev. Mater. Sci.* **16,** 245–261 (1986).

38. Anderson, J. M. & Shive, M. S. Biodegradation and biocompatibility of PLA and PLGA microspheres. *Adv. Drug Deliv. Rev.* **64,** 72–82 (2012).

39. Fattahi, P., Borhan, A. & Abidian, M. R. Characterization of the size, shape, and drug encapsulation efficiency of PLGA microcapsules produced via electrojetting for drug delivery to brain tumors. *Int. IEEE/EMBS Conf. Neural Eng. NER* 953–956 (2013). doi:10.1109/NER.2013.6696093

40. Fattahi, P., Borhan, A. & Abidian, M. R. Microencapsulation of Chemotherapeutics into Monodisperse and Tunable Biodegradable Polymers via Electrified Liquid Jets: Control of Size, Shape, and Drug Release. *Adv. Mater.* **25,** 4555–4560 (2013).